reactions of CrO^+ with cyclopropane and cyclobutane may result from rearrangement and decomposition of the intermediates **27** and **28**, respectively, formed by insertion of CrO^+ in the strained C–C bonds of these cycloalkanes.

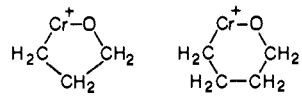

27 **28**

Reaction with cyclopentane eliminates two molecules of H_2 to yield $Cr(C_5H_6O)^+$ exclusively (reaction 25). This multiple dehydrogenation product can be rationalized by a mechanism analogous to Scheme III, which involves initial insertion into a

$$CrO^+ + c\text{-}C_5H_{10} \xrightarrow{91\%} Cr(C_5H_6O)^+ + 2H_2 \quad (25)$$

$$\xrightarrow{9\%} Cr^+ + C_5H_{10}O \quad (26)$$

C–H bond followed by successive β-H transfers to the Cr center to eliminate H_2 (Scheme VII). This mechanism suggests a structure of (C_5H_5)–Cr^+–OH for the double dehydrogenation product. Cyclohexane yields products resulting from dehydrogenation and elimination of H_2O in various intermediate steps.

Summary

1. A single bimolecular encounter between CrO^+ and an alkane provides energetically facile pathways for alkane oxidation. CrO^+ undergoes exothermic reaction with ethane to oxidize ethane into ethanol selectively. In addition to the possibility of alcohol formation, reactions of CrO^+ with larger alkanes provide a variety of product channels for alkane oxidation, which include dehydrogenation and loss of alkenes and smaller alkanes.

2. Reactions of CrO^+ with cyclopropane and cyclobutane yield products characteristic of C–C bond cleavages. Reaction of CrO^+ with cyclopropane is unique, exhibiting a product distribution which closely resembles that of the reaction with propene. In contrast, reactions with cyclopentane and cyclohexane exhibit multiple dehydrogenation and H_2O loss.

3. A CrO^+–H bond dissociation energy of 89 kcal mol^{-1}, determined by examining a series of hydrogen abstraction reactions, implies that the reaction between CrO^+ and an alkyl C–H bond involves multicenter intermediates. This argument, supported by an examination of the reactions of Cr^+ with alcohols, suggests an initial intermediate in which a C–H bond adds across the Cr^+–O bond.

Acknowledgment. We gratefully acknowledge the support of the National Science Foundation under Grant CHE-8407857. Graduate fellowship support by the Korean Government (H.K 1980–1984) is gratefully acknowledged.

Registry No. H_2, 1333-74-0; CrO_2Cl_2, 14977-61-8; Cr, 7440-47-3; $Cr(CO)_6$, 13007-92-6; $Cr(OH)^+$, 68566-23-4; CrO^+, 56371-63-2; $H_2C{=}CHCH_2CH_3$, 106-98-9; *cis*-$H_3CCH{=}CHCH_3$, 590-18-1; $H_2C{=}C(CH_3)_2$, 115-11-7; $H_2C{=}CHCH_3$, 115-07-1; $C_6H_5CH_3$, 108-88-3; $(H_3C)_3CH$, 75-28-5; $H_3CCH_2CH_3$, 74-98-6; $H_3C(CH_2)_2CH_3$, 106-97-8; $(H_3C)_3CCH_3$, 463-82-1; $H_2C{=}CH_2$, 74-85-1; C_6H_6, 71-43-2; $Fe(OH)^+$, 15092-05-4; $Co(OH)^+$, 12323-82-9; CrO, 12018-00-7; CrOH, 36011-51-5; CH_4, 74-82-8; CH_3CH_3, 74-84-0; $HO(CH_2)_2CH_3$, 71-23-8; $H_3CCH(OH)CH_3$, 67-63-0; $H_3CCD_2CH_3$, 2875-95-8; $(H_3C)_2CDCH_3$, 13183-68-1; $D_3C(CH_2)_2CD_3$, 13183-67-0; cyclopropane, 75-19-4; cyclobutane, 287-23-0; cyclopentane, 287-92-3; cyclohexane, 110-82-7.

Mechanistic and Kinetic Study of Alkane Activation by Ti^+ and V^+ in the Gas Phase. Lifetimes of Reaction Intermediates

M. A. Tolbert and J. L. Beauchamp*

Contribution No. 7394 from the Arthur Amos Noyes Laboratory of Chemical Physics, California Institute of Technology, Pasadena, California 91125. *Received May 14, 1986*

Abstract: The reactions of Ti^+ and V^+ with several deuterium-labeled alkanes are studied by using an ion beam apparatus. The dominant reactions observed for both of these metal ions are single and double dehydrogenations. Alkane loss reactions are also observed for Ti^+ but may be due to electronically excited states. The dehydrogenation mechanisms are investigated by using partially deuterated alkanes. The results are consistent with 1,2-eliminations for both V^+ and Ti^+, where deuterium scrambling may occur in the latter case. It is proposed that some 1,3-elimination of hydrogen also occurs in the reaction of Ti^+ with *n*-butane. Although the dehydrogenation reactions of V^+ and Ti^+ appear to be similar to those of Ru^+ and Rh^+, there are some important differences in the reactivity of V^+. Extensive adduct formation and large deuterium isotope effects are consistent with reaction intermediates which are relatively long-lived for V^+ in comparison to Ti^+, Ru^+, and Rh^+. Collisional stabilization studies are used to estimate dissociation rates of reaction intermediates formed when Ti^+ and V^+ interact with *n*-butane. The measured upper limits to the unimolecular decomposition rates are 1.47×10^5 s^{-1} and 1.23×10^7 s^{-1} for V^+ and Ti^+, respectively. Model RRKM calculations are able to reproduce these rates and provide an explanation of isotope effects observed when *n*-butane-d_{10} is employed as the neutral reactant. The slower rate for V^+ is suggested to arise from the inability of V^+ to form two strong σ bonds due to the $3d^4$ electronic configuration of the ground-state ion. This renders C–H bond insertion energetically much less favorable for V^+ than for the other metal ions and limits the excitation energy of reaction intermediates.

Recent studies have indicated that a wide variety of transition-metal ions are capable of activating the bonds of totally saturated hydrocarbons.[1-6] These studies have revealed that, although groups of transition-metal ions exhibit similar reactivity (i.e., Ru^+, Rh^+; Fe^+, Co^+, Ni^+), there are also intriguing dif-

Table I. Bond Dissociation Energies[a]

M^+	$D(M^+ - H)$ exp	$D(M^+ - H)$ theory[b]	$D(M^+ - CH_3)$ exp
Ti^+	55[c]	55.0	56.5[c]
V^+	48[d]	44.5	50[d]

[a] All values in kcal/mol. [b] Reference 36. [c] Reference 7. [d] Reference 8.

(1) (a) Halle, L. F.; Armentrout, P. B.; Beauchamp, J. L. *Organometallics* **1982**, *1*, 963. (b) Armentrout, P. B.; Beauchamp, J. L. *J. Am. Chem. Soc.* **1981**, *103*, 784. (c) Houriet, R.; Halle, L. F.; Beauchamp, J. L. *Organometallics* **1983**, *2*, 1818.
(2) Jacobson, D. B.; Freiser, B. S. *J. Am. Chem. Soc.* **1983**, *105*, 5197.
(3) Halle, L. F.; Houriet, R.; Kappes, M. M.; Staley, R. H.; Beauchamp, J. L. *J. Am. Chem. Soc.* **1982**, *104*, 6293.
(4) Tolbert, M. A.; Mandich, M. L.; Halle, L. F.; Beauchamp, J. L. *J. Am. Chem. Soc.* **1986**, *108*, 5675.

0002-7863/86/1508-7509$01.50/0

Table II. Lower Electronic States of Ti^+ and V^+ and Their Relative Ion Populations at 2500 K

	state	configrtn	energy[a]	rel populatn
Ti^+	^4F	$3d^24s^1$	0.00	0.61
	^4F	$3d^3$	0.11	0.37
	^2F	$3d^24s^1$	0.56	0.02
	^2D	$3d^24s^1$	1.05	<0.01
V^+	^5D	$3d^4$	0.00	0.77
	^5F	$3d^34s^1$	0.34	0.23
	^3F	$3d^34s^1$	1.08	<0.01

[a] State energies in eV are a weighted average over the J states from ref 14.

ferences in reactivity from one metal ion to another. For example, the metal ion mediated dehydrogenation of *n*-butane has been shown to proceed via at least three distinct mechanisms, illustrated in Scheme I. It has been proposed that Sc^+ effects a predominantly 1,3-elimination,[5] resulting in the formation of a metallocyclobutane complex **1**. Dehydrogenation at Ni^+ centers has been shown to occur by a 1,4-elimination mechanism,[3] resulting in the formation of a metal–bisolefin complex **2**. Pd^+ appears to effect a selective 1,2-elimination across the central C–C bond exclusively,[4] forming a monoolefin complex. Although these studies have led to a greater understanding of C–H bond activation processes, it is still not possible to predict, a priori, the mechanisms by which the bonds of alkanes are cleaved by transition-metal ions.

In the present study, we report the reactions of Ti^+ and V^+ with alkanes, with the specific objective of examining the dehydrogenation reactions that occur at these metal ion centers. The bond strengths of H and CH_3 to these metal ions have been reported previously[7,8] and are summarized in Table I. Some of the chemistry of Ti^+ and V^+ with hydrocarbons has been reported previously,[8-12] but these studies have not utilized deuterium-labeled alkanes. Earlier studies in our laboratory have benefited greatly from the use of labeled hydrocarbons.[1c,3-5] In this study, partially deuterated alkanes are used to help elucidate the reaction mechanisms for alkane activation by Ti^+ and V^+. Deuterium isotope effects are explored by studying the reactions with partially and totally deuterated alkanes. The reactivity of Ti^+ and V^+ is compared to that of other transition-metal ions, both early (Sc^+),[5] and late (Fe^+, Co^+, Ni^+, Ru^+, Rh^+, and Pd^+).[1,4] Estimates of the overall decomposition rates are obtained from the pressure dependence of product yields by using buffer gases to stabilize reactive intermediates. The differences in decomposition rates and isotope effects are analyzed by comparison to model RRKM calculations and discussed in terms of the electronic configurations of the metal ions.

Experimental Section

The ion beam apparatus used in the present study has been described previously.[13] Briefly, ion beams of Ti^+ and V^+ are produced by vaporization of $TiCl_4$ and $VOCl_3$ onto a hot rhenium filament and subsequent surface ionization at 2500 K. The excited-state distributions of Ti^+ and V^+ at 2500 K are indicated in Table II.[14] Assuming that the ion internal temperature matches the filament temperature, it can be seen that a substantial portion of the ions is formed in electronically excited states for Ti^+ and V^+, 37% and 23%, respectively. Furthermore, because the transitions between the low-lying states are all parity forbidden, it is expected that the excited-state lifetimes will be quite long.[15] The metal ions are collimated, mass and energy selected, and focussed into a collision chamber containing the neutral reactant at ambient temperature. Product ions scattered in the forward direction are analyzed by using a quadrupole mass spectrometer. The flight time of the metal ions through the apparatus is approximately 10–30 μs, which may be shorter than the excited-state lifetimes of the metal ions. Thus, the reaction observed could be a combination of ground- and excited-state reactions.

Collisional stabilization studies of reactive intermediate ions were performed by adding variable pressures of D_2 and CF_4 as buffer gases. These gases were chosen because they do not react with the species present and are representative of low and high efficiency stabilization gases, respectively. The use of D_2 makes it possible to identify isotopic hydrogen exchange reactions (if they occur). The buffer gases were added to the collision chamber with the reactant gas by using a dual inlet

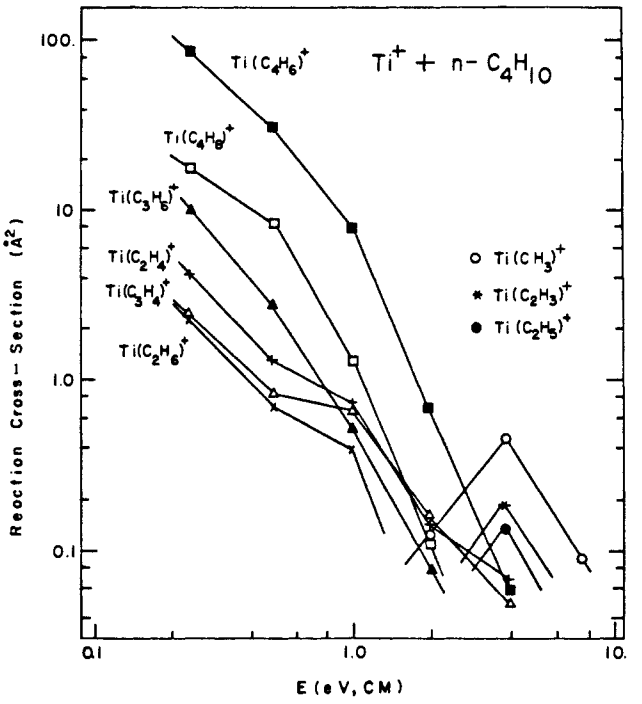

Figure 1. Variation in the experimental cross section for the reaction of Ti^+ and *n*-butane with relative kinetic energy is the center of mass frame. Lines drawn through single data points are extrapolated to lower values at higher and lower energies.

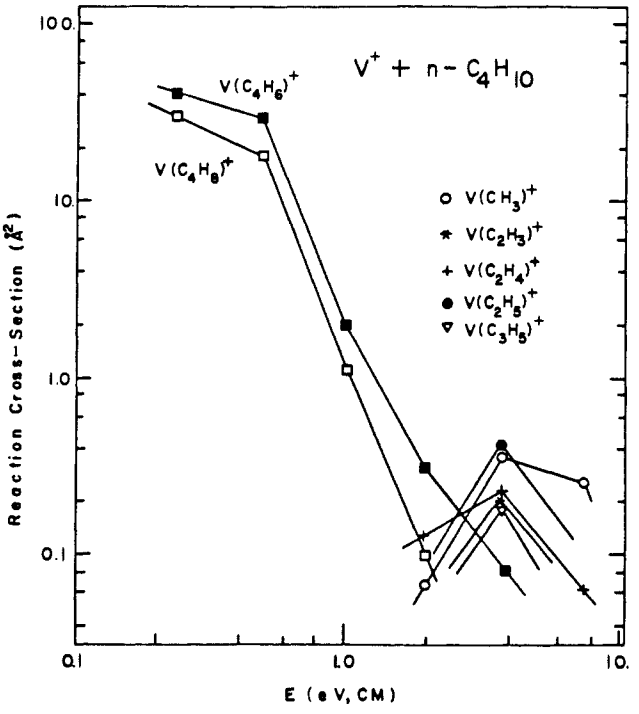

Figure 2. Variation in the experimental cross section for the reaction of V^+ and *n*-butane with relative kinetic energy in the center of mass frame.

(5) Tolbert, M. A.; Beauchamp, J. L. *J. Am. Chem. Soc.* **1984**, *106*, 8117.
(6) Byrd, G. D.; Freiser, B. S. *J. Am. Chem. Soc.* **1982**, *104*, 5944.
(7) Elkind, J. L.; Ervin, K. M.; Aristov, N.; Armentrout, P. B., submitted for publication. Armentrout, P. B., private communication.
(8) Aristov, N.; Armentrout, P. B., submitted for publication.
(9) Byrd, G. D.; Burnier, R. C.; Freiser, B. S. *J. Am. Chem. Soc.* **1982**, *104*, 3565.
(10) Kappes, M. M.; Staley, R. H., unpublished results.
(11) Allison, J.; Ridge, D. P. *J. Am. Chem. Soc.* **1977**, *99*, 35.
(12) Allison, J.; Ridge, D. P. *J. Am. Chem. Soc.* **1978**, *100*, 163.
(13) (a) Armentrout, P. B.; Beauchamp, J. L. *Chem. Phys.* **1980**, *50*, 21. (b) Armentrout, P. B.; Beauchamp, J. L. *J. Chem. Phys.* **1981**, *74*, 2819.
(14) Moore, C. E. *Atomic Energy Levels*. National Bureau of Standards: Washington DC, 1949.
(15) Garstang, R. H. *Monthly Notice Royal Astron. Soc.* **1962**, *124*, 321.

Scheme I

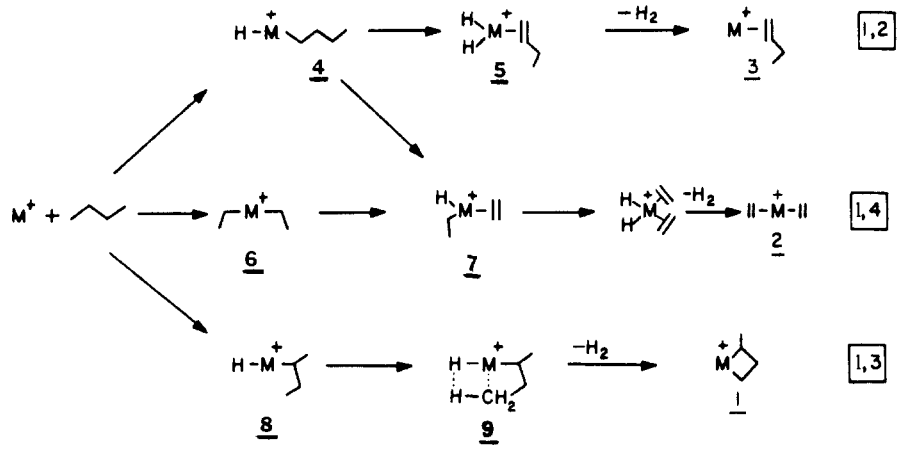

Table III. Product Distributions for the Reactions of Ti^+ and V^+ with Alkanes at a Relative Kinetic Energy of 0.5 eV[a]

		Ti^+		V^+		
alkane	neutral prods.	ion beam	ICR[b]	ion beam	ICR[c]	σ max[d]
C_2H_6	H_2	0.96	1.0	1.0	no reactn	
	$2H_2$*	0.04				
	σ tot.[e]	5.2		0.9		50
C_3H_8	H_2	0.94	1.0	1.0	1.0	
	$2H_2$*	0.03				
	CH_4	0.03				
	σ tot.	55		13		60
n-C_4H_{10}	H_2	0.17		0.39		
	$2H_2$	0.66	1.0	0.61		
	CH_4	0.09		tr[f]		
	$CH_4 + H_2$	0.03				
	C_2H_4	0.02				
	C_2H_6	0.03		tr		
	σ tot.	45		48		68
i-C_4H_{10}	H_2	0.90	0.84	1.0		
	$2H_2$	0.06	0.16			
	CH_4	0.02				
	$CH_4 + H_2$	0.01				
	C_2H_4	0.01				
	σ tot.	154		65		68
2,2-dimethylpropane	H_2	0.54	0.22			
	$2H_2$	0.05	0.16			
	CH_4	0.15		0.76		
	$CH_4 + H_2$	0.26	0.62	0.24		
	σ tot.	73		3.0		75
2,2,3,3-tetramethylbutane	$2H_2$	0.70		0.67		
	$CH_4 + H_2$	0.11				
	$C_2H_6 + H_2$	0.09				
	C_3H_8	0.05				
	$C_3H_8 + H_2$	0.01				
	C_4H_{10}	0.03		0.33		
	$C_4H_{10} + H_2$	0.01				
	σ tot.	141		30		94

[a] Reaction products which exhibit reaction thresholds characteristic of endothermic processes are indicated by an asterisk. [b] Reference 9. [c] Reference 10. [d] Maximum cross section predicted from the encounter rate based on an ion interacting with a polarizable neutral: Gioumousis, G.; Stevenson, D. P. *J. Chem. Phys.* **1958**, *29*, 294. Polarizabilities from Chan, S. C.; Rabinovitch, B. S.; Bryant, J. T.; Spicer, L. D.; Fujimoto, Y. N.; Pavlou, S. P. *J. Phys. Chem.* **1970**, *24*, 3160. Cross secctions in A^2. [e] Total reaction cross section are ±50%, in $Å^2$. The total reaction cross section reported does not include any adduct ions formed. Since adduct formation (which is often pronounced for V^+) occurs at the expense of the observed product intensities, these total cross sections should be regarded as lower limits to the actual values. [f] Present in trace amounts, <1% of the total product distribution.

system. The buffer gas pressures used in these experiments ranged from 1 to 20 mtorr as measured by using a capacitance manometer.

Deuterium-labeled CH_3CD_3 (98 %D), propane-*2,2*-d_2 (98 %D), propane-d_8 (98.5 %D),*n*-butane-*1,1,1,4,4,4*-d_6 (98 %D), *n*-butane-d_{10} (98.5 %D), and 2-methylpropane-*2*-d_1 (98 %D) were obtained from Merck, Sharp and Dohme.

Results

Both Ti^+ and V^+ react with alkanes to form a variety of products. Although the major products of these reactions are quite similar, there are substantial differences in the minor products. For example, the cross section behavior for the reactions of Ti^+ and V^+ with *n*-butane is illustrated in Figures 1 and 2, respectively. The exothermic reactions are easily identified since their cross sections decrease with increasing relative kinetic energy. It can be seen that the two most prominent exothermic processes for Ti^+ and V^+ reacting with *n*-butane are the same, namely, loss of one and two molecules of H_2. However, the reaction of Ti^+ with *n*-butane also results in a variety of minor exothermic products not observed for V^+. This trend is true in general for the reactions of Ti^+ and V^+ with alkanes.

Product distributions and overall cross sections for the reactions of Ti^+ and V^+ with alkanes at a relative kinetic energy of 0.5 eV are given in Table III. Also included in this table are previous results from ion cyclotron resonance (ICR) experiments.[9,10] The

Table IV. Adduct Formation in the Reactions of Transition-Metal Ions with Alkanes[a]

	Sc^+[b]	Ti^+	V^+	Fe^+[c]	Co^+[c]	Ni^+[c]	Ru^+[c]	Rh^+[c]	Pd^+[c]
C_2H_6	0	0.01	0.25	ns[d]	ns	ns	0	0	ns
C_3H_8	0	0.01	0.32	0.42	0.39	0.25	0	0	0.35
n-C_4H_{10}	0	0.01	0.28	0.05	0.07	0.06	0	0	0.57
i-C_4H_{10}	0	0.01	0.27	0.05	0.07	0.09	0	0	0.23
2,2-dimethylpropane	0.10	0.18	0.97	0.04	0.02	0.10	0	0	0.31

[a] Fraction of the total product observed, normalized to 1.0, at a relative kinetic energy of 0.5 eV in the center of mass frame. The pressure of alkane gas was 1.5 m torr in each case. [b] Tolbert, M. A.; Beauchamp, J. L., unpublished results. [c] Reference 4. [d] Not studied. [e] Halle, L. F.; Armentrout, P. B.; Tolbert, M. A., unpublished results.

Table V. Isotopic Product Distributions for Dehydrogenation of Deuterated Alkanes by Ti^+ and V^+ at a Relative Kinetic Energy of 0.5 eV

		single dehydrogenation			double dehydrogenation			
M^+	alkane	H_2	HD	D_2	$2H_2$	H_2 + HD	2HD or H_2 + D_2	D_2 + H_2
Ti^+	CH_3CD_3	0.05	0.91	0.04				
	$CH_3CD_2CH_3$	0.07	0.93					
	$(CH_3)_3CD$	0.12	0.88		0.66	0.64		
	$CD_3CH_2CH_2CD_3$	0.10	0.90		0.07[a]	0.25	0.55	0.13
V^+	CH_3CD_3		1.0[b]					
	$CH_3CD_2CH_3$		1.0					
	$(CH_3)_3CD$		1.0					
	$CD_3CH_2CH_2CD_3$	0.71	0.29			0.15	0.67	0.18

[a] The identity of this product is uncertain due to the identical masses of D_2 and $2H_2$. To make the product distributions best match those in Table III, all of this mass product was assigned to be $2H_2$. [b] Reference 8.

Table VI. Isotopic Product Distributions for Hydrocarbon Loss from Deuterated Alkanes by Ti^+ at a Relative Kinetic Energy of 0.5 eV

alkane	CH_4	CH_3D	CH_2D_2	CHD_3	CD_4	$C_2H_2D_4$	$C_2H_3D_3$	C_2H_4	C_2HD_3
$CH_3CD_2CH_3$	0.68	0.32							
$(CH_3)_3CD$	0.81	0.19							1.0
$CD_3CH_2CH_2CD_3$		0.06	0.09	0.53	0.32	0.59	0.41	1.0	

major products in most cases are similar, by using the two methods. However, our study finds a number of minor products not reported previously for Ti^+. There are two possible explanations for the differences. First, it is possible that these products were overlooked in the earlier study because they comprise such a small fraction of the product distribution. No products were reported in the earlier study that had an abundance of less than 4% of the total product. A second possibility is that the minor processes we observe are due to electronically excited-state ions. This may certainly be the case. However, it is expected that excited-state ions would be as abundant or even more so in the ICR studies because the ions are created by electron impact ionization of volatile organometallic precursors at 70 eV. Ions created in this way have previously been shown to be formed with a high degree of electronic as well as translational excitation.[16-18] The possibility that different electronically excited states are accessed by the two methods of ion formation could account for some of the observed differences.

As mentioned above, the minor products in the reactions of Ti^+ and V^+ might very well be due to electronically excited states. This would result in the observed cross sections being combinations of exothermic excited-state reactions and endothermic ground-state reactions. This type of cross section behavior was recently reported for the reaction of V^+ with ethane.[8] The authors concluded that the exothermic reaction was due entirely to excited-state V^+. Our results for the reaction of V^+ with C_2H_6 are in agreement with these previous results. We observe other reactions for V^+ which may be due solely to excited-state reactions. For example, the reaction of V^+ with 2,2-dimethylpropane forms two products, but the total reaction cross section is extremely low, only 3 A^2 at a relative kinetic energy of 0.5 eV (Table III). It is very likely that both of these products are due entirely to excited-state reactions and that the ground state of V^+ does not undergo any exothermic reactions with 2,2-dimethylpropane.

In addition to the reaction products indicated in Table III, adducts of the reactant metal ions with the parent hydrocarbon are often observed in the ion beam experiment at low relative kinetic energies. In the present experiments, only the masses of the ions are measured. No structural information about the adduct ions is obtained. Thus, the term adduct is used to indicate a species with the combined mass of the metal ion and the parent hydrocarbon, and does *not* imply any particular structure. As mentioned previously, the flight time through the collision chamber and detector is approximately 10–30 μs. Thus, adducts with lifetimes in this range will be detected directly in the present experiment. At pressures of 1.5 mtorr, the time between collisions is also approximately 10 μs. Thus, adducts which live 10 μs have the possibility of suffering a second collison. This could lead to stabilization of the adduct ion which might then live long enough to be detected. The extent of adduct formation for Ti^+ and V^+ reacting with alkanes is indicated in Table IV, along with previous results for other metal ions. It can be seen that, although similar products are formed in the reactions of Ti^+ and V^+, the extent of adduct formation is dramatically different for the two metal ions. Whereas adducts of Ti^+ are only a very small fraction of the total product, V^+ reactions are characterized by extensive adduct formation. In fact, adducts make up over 97% of the total products for the reactions of V^+ with 2,2-dimethylpropane. This indicates that the lifetimes of the adducts of V^+ are much longer than the corresponding adducts of the other metal ions, with the exception of Pd^+. It should be noted that, in agreement with our findings, recent studies by Weisshaar et al. found no adducts of Ti^+ with propane in a high-pressure flow reactor containing 1 torr of He.[19]

In order to gain insight into the specific reaction mechanisms, the reactions of Ti^+ and V^+ with deuterium-labeled alkanes were studied. The results for the exothermic dehydrogenations of labeled alkanes at a relative kinetic energy of 0.5 eV are given in Table V. The results for the alkane loss reactions are presented in Table VI.

As indicated in Table III, a minor product observed in the reaction of Ti^+ with n-butane is $Ti(C_2H_6)^+$. With the use of labeled n-butane-*1,1,1,4,4,4-d_6*, it is seen that this product cor-

(16) Halle, L. F.; Armentrout, P. B.; Beauchamp, J. L. *J. Am. Chem. Soc.* **1981**, *103*, 962.
(17) Freas, R. B.; Ridge, D. P. *J. Am. Chem. Soc.* **1980**, *102*, 7129.
(18) Kang, H.; Beauchamp, J. L. *J. Phys. Chem.* **1985**, *89*, 3364.
(19) Tonkyn, R.; Weisshaar, J. C. *J. Phys. Chem.*, submitted for publication.

Table VII. Comparison of the Reactions of Transition-Metal Ions with *n*-Butane at a Relative Kinetic Energy of 0.5 eV

neutral prod	Sc^{+} [a]	Ti^{+}	V^{+}	Fe^{+} [b]	Co^{+} [c]	Ni^{+} [d]	Ru^{+} [e]	Rh^{+} [e]	Pd^{+} [e]
H_2	0.37	0.17	0.39	0.20	0.29	0.48	0.20	0.27	0.38
$2H_2$	0.22	0.66	0.61				0.80	0.73	
CH_4	0.01	0.09		0.41	0.12	0.06			0.21
$CH_4 + H_2$	0.02	0.03							
C_2H_4	0.36	0.02							
C_2H_6	0.02	0.03		0.39	0.59	0.45			0.41
σ tot.	103	45	48	98	170	88	38	48	29

[a] Reference 5. [b] Reference 1 and Halle, L. F. and Beauchamp, J. L., unpublished results. [c] Reference 1b. [d] Reference 3. [e] Reference 4.

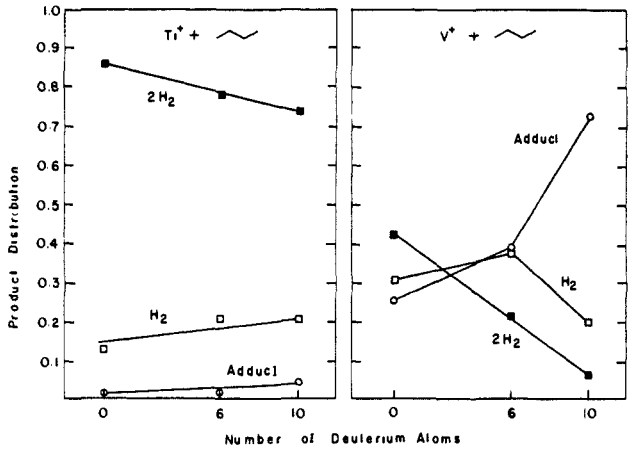

Figure 3. Product distribution for the dehydrogenation of *n*-butane by Ti^{+} and V^{+} as a function of the extent of deuteration. The single and double dehydrogenation processes are referred to as H_2 and $2H_2$, respectively, regardless of the deuterium label.

responds to $Ti(C_2D_6)^{+}$. This suggests a dimethyl species similar to that proposed previously for Sc^{+}.[5] If formation of this product is due to ground-state Ti^{+}, then observation of this process as an exothermic reaction indicates that the sum of the first and second metal–methyl bond energies is greater than 112 kcal/mol.[20] Using the previous value for the first titanium methyl bond (Table I) implies $D(TiCH_3^{+}-CH_3) \geq 56$ kcal/mol.

In the reaction of V^{+} with *n*-butane-*1,1,1,4,4,4-d*$_6$, it was observed that the product distribution was different than for unlabeled *n*-butane. To investigate this further, the reactions of Ti^{+} and V^{+} with totally deuterated alkanes, i.e., with *n*-butane-d_{10} and propane-d_8, were studied. The product distributions for the dehydrogenation reactions of Ti^{+} and V^{+} with *n*-butane as a function of deuteration are illustrated in Figure 3. It can be seen that for both metal ions, as the extent of deuteration increases, the extent of double dehydrogenation decreases relative to single dehydrogenation and adduct formation. This effect is markedly pronounced; however, in the reaction with V^{+}, where for labeled *n*-butane, the dominant process is no longer loss of $2H_2$ but rather formation of the adduct ion. The *total apparent* cross sections for formation of the adduct *and* the dissociation products are 93 Å^2 for *n*-butane and 90 Å^2 for *n*-butane-d_{10} at 0.25 eV relative kinetic energy. These values are equal, within experimental error, to the calculated collision cross section (see Table III) of 96 Å^2 at this energy. The higher yield of dissociation products (2.5 times larger) with *n*-butane compared to *n*-butane-d_{10} under identical experimental conditions directly reflects the longer lifetimes of the adduct in the latter case. A large isotope effect is also observed in the reactions of V^{+} with propanes. Although adduct formation is 32% of the total product for propane (Table III), it is 70% of the total product for propane-d_8.

In an attempt to understand the source of the large isotope effect observed, the pressure dependence of the reactions of Ti^{+} and V^{+} with *n*-butane were studied by using D_2 and CF_4 as stabilizing gases. For the reaction of V^{+} with C_4H_{10}, it was found that both

(20) Auxiliary heats of formation from Cox, J. D.; Pilcher, G. "Thermochemistry of Organic and Organometallic Compounds"; Academic Press: New York, 1970. $\Delta H_f(CH_3) = 35.1$ from ref 35.

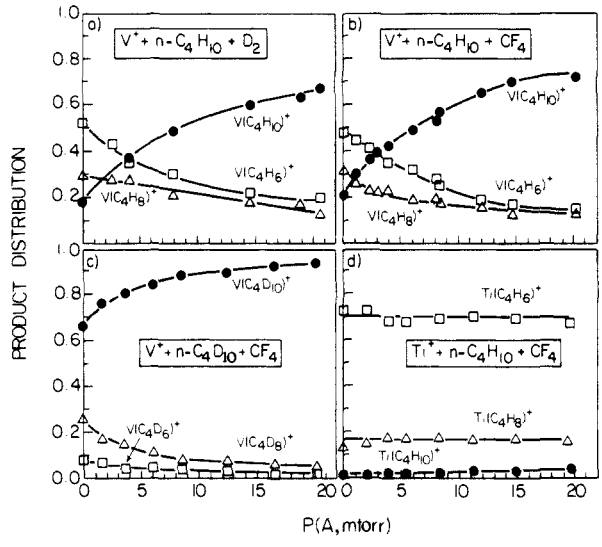

Figure 4. Product distributions as a function of buffer gas pressure at a relative kinetic energy of 0.25 eV for the reaction of (a) V^{+} with *n*-butane, A = D_2, (b) V^{+} with *n*-butane, A = CF_4, (c) V^{+} with *n*-butane-d_{10}, A = CF_4, and (d) Ti^{+} with *n*-butane, A = CF_4.

D_2 and CF_4 could effectively stabilize the adduct, making adduct formation the dominant process at high pressures as shown in Figure 4 (parts a and b, respectively). Adduct stabilization by CF_4 was also observed in the reaction of V^{+} with C_4D_{10}, Figure 4c. In contrast, attempts to collisionally stabilize $Ti(C_4H_{10})^{+}$ did not result in a substantial change in the observed product distribution as shown in Figure 4d.

Discussion

The reactions of Ti^{+} and V^{+} with hydrocarbons are dominated by the loss of one or more molecules of hydrogen. In addition, smaller amounts of alkane loss products are observed for Ti^{+}. A comparison of the reactions of transition-metal ions with *n*-butane is given in Table VII. It can be seen that the major reactions of Ti^{+} and V^{+} are *not* analogous to those of the remaining first-row transition-metal ions. Instead, there is a similarity, perhaps superficial, to the reactivity of the second-row ions Ru^{+} and Rh^{+}. Although the reactivity appears to be quite similar, there are substantial differences as well. For example, adduct ions are very abundant in the reactions of V^{+} but are not observed at all for Ru^{+} and Rh^{+} (Table IV). Furthermore, although no alkane loss products are observed in the reactions of V^{+}, these reactions are observed in certain circumstances for Ru^{+} and Rh^{+}. Other clues that provide an understanding of the reactivity of V^{+} and Ti^{+} may be obtained from an examination of the dehydrogenation mechanisms and deuterium isotope effects that occur in the reactions of these metal ions. In addition, the similarities and differences in reactivity among the various metal ions can be explained in part in terms of the electronic configuration of the metal ions and the corresponding bonding configurations.

Dehydrogenation Mechanisms for Ti^{+} and V^{+}. Remarkable metal ion specificity has been observed in the dehydrogenation reactions of alkanes at transition-metal ion centers. These reactions have been studied by using a variety of techniques. These include deuterium labeling studies,[1c,3-5] product structural determinations using collision-induced dissociation,[21-23] and kinetic

Table VIII. Comparison of Dehydrogenation Products and Proposed Mechanisms for Transition-Metal Ions Reacting with *n*-Butane-1,1,1,4,4,4-d_6

	Sc^{+a}	Ti^+	V^+	Fe^{+b}	Co^{+c}	Ni^{+c}	Ru^{+d}	Rh^{+d}	Pd^{+d}
H_2		0.10	0.71	0.59	0.18		0.20	0.32	1.0
HD	1.0	0.90	0.29	0.18	0.31		0.46	0.61	
D_2				0.23	0.51	1.0	0.34	0.07	
proposed mechansm	1,3	1,2, 1,3	1,2	1,4, 1,2	1,4	1,4	1,2	1,2	1,2

[a] Reference 5. [b] References 1 and 26. [c] References 1, 2, 24, and 25. [d] Reference 4.

Scheme II

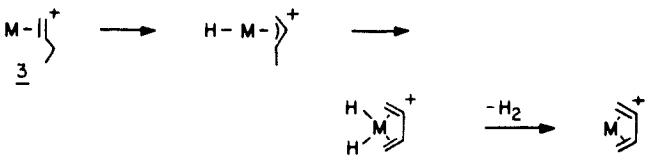

energy release distribution (KERD) measurements.[24-26] The results have indicated that dehydrogenation of alkanes smaller than *n*-butane by Fe^+, Co^+, Ni^+, Ru^+, Rh^+, and Pd^+ proceed via a 1,2-process where hydrogens from adjacent carbons are eliminated. With alkanes larger than *n*-butane where a 1,4-process can occur, it is the predominant reaction in the case of Fe^+, Co^+, and Ni^+. In contrast, hydrogen elimination at Sc^+ centers has been proposed to occur via a 1,3-process wherein a metallocyclobutane complex is formed and H_2 is eliminated via a 4-center transition state.[5]

The reactions of V^+ with small alkanes are consistent with a predominantly 1,2-elimination mechanism. For example, as indicated in Table V, HD loss is the only process observed in the reactions with deuterated alkanes smaller than *n*-butane. The reactions of Ti^+ are somewhat more complicated. The major dehydrogenation products for Ti^+ are also consistent with a 1,2-elimination mechanism. However, as indicated in Table V, small amounts of H_2 elimination occur from CH_3CD_3, propane-*2,2*-d_2, and 2-methylpropane-*2*-d_1. These could be a result of scramling or could be due in the case of the propanes to a 1,3-elimination mechanism similar to that inferred for Sc^+. These two different processes cannot be distinguished in this experiment. KERD measurements could perhaps distinguish between the 1,2- and 1,3-elimination mechanisms.

As mentioned previously, a great deal of interest and attention has recently been paid to the dehydrogenation mechanisms of *n*-butane by transition-metal ions (Scheme I). A summary of the products observed by using labeled *n*-butane-*1,1,1,4,4,4*-d_6 and the proposed dehydrogenation mechanism for the various metal ions studied to date is presented in Table VIII. Note that each metal ion, including Ti^+ and V^+, reacts in a quite distinct manner.

The reaction with Ti^+ results in a large amount of HD loss, second only to that observed for Sc^+. It is thus possible that a combination of a 1,2- and 1,3-dehydrogenation mechanism is operative in the reactions of Ti^+ with *n*-butane. It is possible that Ti^+ preferentially inserts into the tertiary or secondary C–H bonds of alkanes. This would prevent abundant 1,3-eliminations of H_2 from propane and 2-methylpropane because only β-hydrogens are available after initial C–H bond insertion. However, in the case of *n*-butane, secondary C–H bond insertion can be followed by either β-H or γ-H transfer. If γ-H transfer occurs, a metallocyclobutane complex is formed which probably cannot undergo subsequent hydrogen elimination. If, instead, β-H transfer occurs, the metal–olefin product formed, **3**, may undergo subsequent hydrogen elimination via allylic hydrogen transfers as indicated in Scheme II. This is consistent with the experimental observations that the major single dehydrogenation product is HD, whereas the major double dehydrogenation product is 2HD (H_2 + D_2). Note that double dehydrogenation is the dominant process at low energies (Figure 1), which suggests that β-H transfers are more facile than γ-H transfers. This also explains the prominent loss of H_2 from 2,2-dimethylpropane. In this reaction, after C–H bond insertion, no β-hydrogens are available for transfer. This allows the transfer of less competitive groups, such as γ-hydrogens or methyl groups. The occurrence of 1,3-eliminations for Ti^+ is also supported by the fact that other reactions of Ti^+ with *n*-butane are similar to Sc^+. For example, formation of $M(C_2H_6)^+$ observed here for Ti^+ is the major product in the reaction of Sc^+ with *n*-butane and is not observed at all for the other first-row transition-metal ions.

The reaction of V^+ with labeled *n*-butane-*1,1,1,4,4,4*-d_6 results in the prominent elimination of H_2. The product distribution observed for V^+ is similar to that of Pd^+, where only H_2 loss is observed. The mechanism proposed for dehydrogenation by Pd^+ involves hydride abstraction as the first step, leaving a carbonium ion to interact with the metal center.[4] The product distribution observed for V^+ is consistent with a 1,2-mechanism, where the secondary C–H bonds are preferentially attacked. Note that this mechanism is probably *not* initiated by hydride abstraction due to the much lower hydride affinity of V^+, 176 kcal/mol,[27] relative to Pd^+, 231 kcal/mol.[28] It should also be noted that an isotope effect could account for the preferential loss of H_2 from *n*-butane-*1,1,1,4,4,4*-d_6 by V^+.

The dehydrogenation mechanisms for V^+ and Ti^+ thus appear to be somewhat similar to those proposed for Ru^+ and Rh^+. The products observed are consistent with predominantly 1,2-eliminations from small alkanes. The reaction of Ti^+ with *n*-butane, however, appears to result in some 1,3-elimination not observed in the reactions of Ru^+ or Rh^+. The scrambling observed in the reactions of Ti^+ may be explained by either a 1,3-elimination or reversible β-H transfers or both. A difference in the reactivity of V^+ as compared to Ti^+, Ru^+, and Rh^+ is that no deuterium scrambling occurs in the V^+ reactions. This indicates that reductive elimination of H_2 competes effectively with olefin insertion into the M–H bond at V^+ centers. Note that this is not the case for Ti^+, where scrambled products are observed in the dehydrogenation reactions. Other previous results have indicated that olefins can easily insert into the Ti^+–CH_3 bond.[29] This is in agreement with our findings of scrambled products for Ti^+. Olefin insertion processes are also thought to be facile at Ru^+ and Rh^+ centers.[4,30]

Comparison of Alkane Loss Reactions for Transition-Metal Ions. As evident from Table VII, the major reactions of Ti^+ and V^+ are quite similar to those observed with Ru^+ and Rh^+. The major reactions involve the loss of one or two molecules of H_2. Alkane loss reactions occur with fairly low cross section for Ti^+ and may be due to electronically excited Ti^+. These products are not observed as exothermic processes for V^+ at all. As discussed in

(21) Jacobson, D. B.; Freiser, B. S. *J. Am. Chem. Soc.* **1983**, *105*, 736.
(22) Larsen, B. S.; Ridge, D. P. *J. Am. Chem. Soc.* **1984**, *106*, 1912.
(23) Peake, D. A.; Gross, M. L.; Ridge, D. P. *J. Am. Chem. Soc.* **1984**, *106*, 4307.
(24) Hanratty, M. A.; Beauchamp, J. L.; Illies, A. J.; Bowers, M. T. *J. Am. Chem. Soc.* **1985**, *107*, 1788.
(25) Hanratty, M. A.; Beauchamp, J. L.; Illies, A. J.; van Koppen, P.; Bowers, M. T. *J. Am. Chem. Soc.*, submitted for publication.
(26) van Koppen, P.; Jacobson, D. B.; Beauchamp, J. L.; Bowers, M. T., to be submitted.
(27) The hydride affinity of V^+ is 176 kcal/mol, calculated from the value $D(V^+-H)$ = 37.9 kcal/mol from sallans, L.; Lane, K.; Squires, R. R.; Freiser, B. S. *J. Am. Chem. Soc.* **1985**, *107*, 4379.
(28) Tolbert, M. A.; Beauchamp, J. L. *J. Phys. Chem.*, submitted for publication.
(29) Uppal, J. S.; Johnson, D. E.; Staley, R. H. *J. Am. Chem. Soc.* **1981**, *103*, 508.
(30) Jacobson, D. B.; Freiser, B. S., submitted for publication in *J. Am. Chem. Soc.*

Scheme III

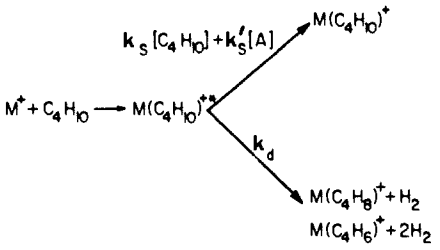

previous work, C–C bond insertions do not occur competitively with C–H insertions at Ru^+ and Rh^+ centers.[4] Similarly, β-alkyl transfers do not occur competitively with β-H transfers for these metal ions.[4] From the observed reactivities, it appears that these same considerations may also apply to Ti^+ and V^+. However, there are some important differences in the reactions of V^+.

A major difference in the reactivity of V^+ relative to Ti^+, Ru^+, and Rh^+ can be seen in the reaction with 2,2-dimethylpropane. After C–H bond insertion at these metal ion centers, no β-hydrogens are available, which makes possible the transfer of less favorable groups, such as a β-methyl group. Thus, Ti^+, Ru^+, and Rh^+ react with 2,2-dimethylpropane to lose CH_4 with quite large cross sections. This suggests that β-alkyl transfers are energetically feasible for these metal ions, even though they are unable to compete with β-hydrogen transfer. The case for V^+, however, is quite different. As discussed previously, ground-state V^+ does not react with 2,2-dimethylpropane at all. The only major product observed in this reaction is the formation of the adduct ion. Thus, if primary C–H bond insertion occurs, it is not followed by β-methyl transfer and alkane elimination. This may indicate that β-methyl transfer is not merely noncompetitive but rather energetically unfeasible. Another explanation for the lack of reactivity is that primary C–H bond insertions do not occur for V^+. This possibility is discussed below.

Lifetimes of Intermediates in the Reactions of V^+ and Ti^+ with *n*-Butane. The reaction of V^+ with alkanes leads to extensive formation of adduct ions (Table IV). As mentioned previously, this indicates that the adduct lifetimes are at least 10 μs. In contrast, no adducts are observed for Ru^+ and Rh^+, even at elevated pressures. Adducts are formed to only a very small extent in the reactions of Ti^+. The adduct ions detected in the reactions of V^+ may have any of a number of different structures, as indicated by intermediates **4–9** in Scheme I. Alternatively, the adduct ion may be the initially formed collision complex, held together by ion-induced dipole interactions or weak acid–base interactions. At higher pressures, collisional stabilization may result in the formation of adduct ions, as indicated in Scheme III for the case of a metal ion interacting with *n*-butane. In this scheme, the initially formed adduct may be collisionally stabilized by a buffer gas, A, or by the *n*-butane itself, with rates constants $k_s'[A]$ and $k_s[C_4H_{10}]$, respectively. Alternatively, the internally excited adduct ion may undergo unimolecular decomposition to a variety of products. The decomposition products will be considered together and are formed with a rate constant k_d.

The ratio of stabilized adducts, S, to decomposition products, D, is given by eq 1. Plots of S/D as a function of buffer gas

$$S/D = (k_s/k_d)[C_4H_{10}] + (k_s'/k_d)[A] \quad (1)$$

pressure are illustrated in Figure 5. The decomposition rates, k_d, may be estimated from the slopes of the lines if the stabilization rate constants, k_s', are known. An upper limit to the stabilization rate constants can be obtained by using the strong collision approximation which assumes that each collision leads to stabilization of the adduct. The collision rate constants are calculated by using eq 2,[31] where α is the polarizability of the buffer gas and μ is the

$$k_s' = 2\pi e(\alpha/\mu)^{1/2} \quad (2)$$

reduced mass of the collision pair. The calculated stabilization

(31) Gioumousis, G.; Stevenson, D. P. *J. Chem. Phys.* **1958**, *29*, 294.

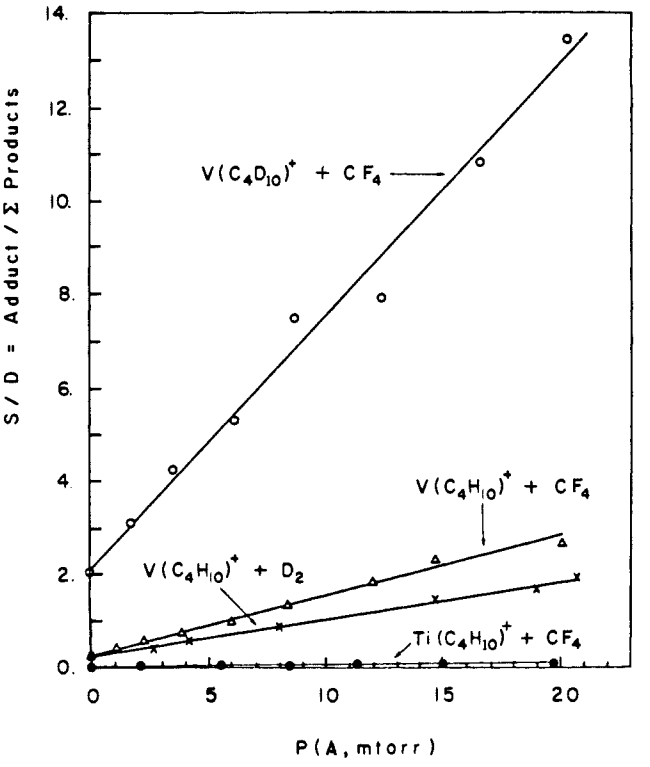

Figure 5. Ratio of stabilized adducts to dissociation products as a function of buffer gas pressure for the reactions of V^+ and Ti^+ with *n*-butane.

Table IX. Rate Constants for Stabilization and Dissociation of $M(n\text{-butane})^+$

adduct	stabilztn gas	k_s'[a] cm³ molecule⁻¹ s⁻¹	k_d[b] s⁻¹
$V(C_4H_{10})^+$	D_2	1.06×10^{-9}	4.65×10^5
	CF_4	5.67×10^{-10}	1.47×10^5
$V(C_4D_{10})^+$	CF_4	5.56×10^{-10}	3.29×10^4
$Ti(C_4H_{10})^+$	CF_4	5.71×10^{-10}	1.23×10^7

[a] Upper limit calculated by using the strong collision assumption, eq 2. [b] Upper limit using k_s' and the slopes of the lines of Figure 5.

rate constants are summarized in Table IX. Using these values in conjunction with the slopes of the lines of Figure 5 yields an *upper limit* to the decomposition rates. These values are also included in Table IX.

An examination of Table IX reveals several important points. First, by using CF_4 as the stabilizing gas, it is seen that the decomposition rate of $Ti(C_4H_{10})^+$ is almost 100 times faster than the decomposition rate of $V(C_4H_{10})^+$. This explains why adduct ions are so prevalent in our experiment for V^+ but not Ti^+. The reaction rates at Ti^+ centers are much faster than the flight time to the detector, and thus few titanium adduct ions are detected.

A second important point to note is that the decomposition rate for V^+ interacting with deuterium-labeled *n*-butane-d_{10} is approximately 4.5 times slower than for undeuterated *n*-butane. Thus the adduct lifetime of $V(C_4D_{10})^+$ is much longer than for $V(C_4H_{10})^+$. Because the lifetimes of the V^+ adducts are comparable to the ion flight time to the detector (10 μs), an increase in adduct lifetime is mirrored by an increase in adduct signal for *n*-butane-d_{10}, as illustrated in Figure 3. The case for Ti^+, however, is quite different. As mentioned previously, the adduct lifetimes for Ti^+ are much shorter than for V^+. Thus, an increase in the lifetime of the titanium adducts upon deuteration might go undetected in our experiment. The reactions are still so fast for Ti^+, even by using deuterium-labeled alkanes, that they are over before the adducts can reach the detector.

A final point to notice in Table IX relates to the relative stabilization efficiencies of the buffer gases D_2 vs. CF_4. The unimolecular decomposition rate constant, k_d, should be independent

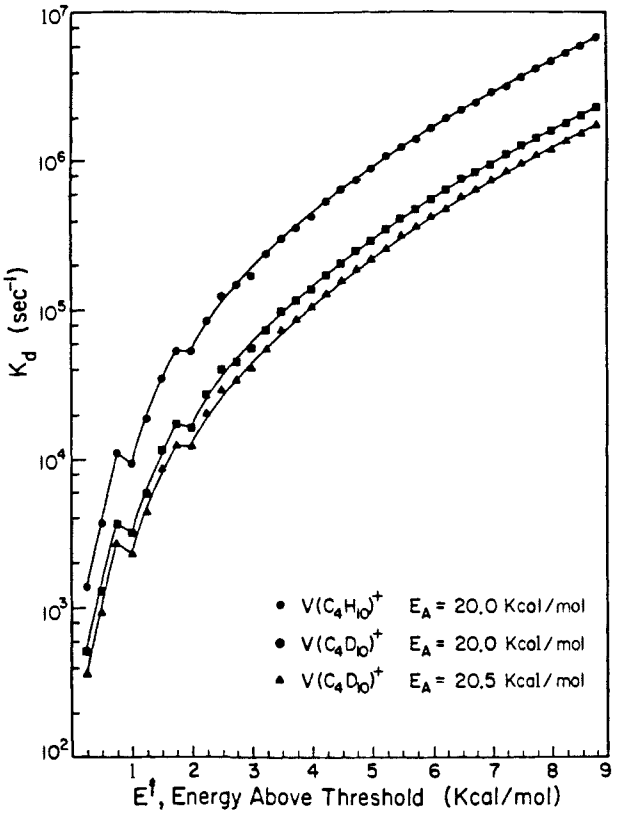

Figure 6. Calculated unimolecular dissociation rates for $V(C_4H_{10})^+$ and $V(C_4D_{10})^+$ as a function of energy above threshold assuming an activation energy of 20 and 20.5 kcal/mol.

of the buffer gas used for its determination. Therefore, differences in the slopes of the lines of Figure 5 give an indication of the relative stabilization efficiencies of D_2 and CF_4. It can be seen that CF_4 is approximately 3.2 times more efficient at stabilizing $V(C_4H_{10})^+$ than is D_2. This is in excellent agreement with the ratio of stabilization efficiencies obtained for the stabilization of $C_5H_9^+$ by CF_4 vs. D_2, namely 3.4.[32]

RRKM Calculations of Unimolecular Dissociation Rates. The decomposition rates of $V(C_4H_{10})^+$ and $V(C_4D_{10})^+$ can be treated by using standard techniques of RRKM theory.[33] The unimolecular rate of dissociation, $k_d(E)$, of $V(C_4H_{10})^+$ is given by eq 3 where E is the internal energy of the energized molecule, E^*

$$k_d(E) = W(E^*)/h\rho^*(E) \quad (3)$$

is the internal energy of the activated complex given by $E - E_0$, E_0 is the activation energy, $W(E^*)$ is the sum of states of the activated complex up to an energy E^*, and $\rho^*(E)$ is the density of states of the energized molecule at an energy E. In the present calculation, $\rho^*(E)$ was calculated by using the Whitten–Rabinovitch approximation and $W(E^*)$ was determined by using a direct state count.

As will be discussed below, the rate-limiting step in the decomposition is likely to be the initial 3-center C–H (C–D) bond insertion step. The frequency factor for this process was taken to be 10^{13} s^{-1} for *both* labeled and unlabeled *n*-butane. The vibrational frequencies were estimated by using the known frequencies of *n*-butane.[34] For $V(C_4D_{10})^+$, the vibrational frequencies were lowered for those vibrations involving motion of the hydrogen atoms for both the energized molecule and the activated complex. The activation energy (assumed to be the same for *both* labeled and unlabeled reactants) and E^* were varied to obtain dissociation rates that were comparable to those estimated in the previous section.

The results for an activation barrier of 20 kcal/mol are illustrated in Figure 6. It can be seen that for all energies above threshold, the rate of bond insertion is approximately three times faster for undeuterated adduct than for deuterated adduct. This is consistent with the experimental observation of longer lived adducts for the deuterated species. This isotope effect is a *general phenomenon* and results from differences in the consequences which deuterium substitution has for the quantities $W(E^*)$ and $\rho^*(E)$ in eq 3. Similar behavior has been observed previously. For example, a large isotope effect was observed in the dissociation reaction of $C_5H_9^+$ and $C_5D_9^+$ to lose H_2 and D_2, respectively.[35] The latter case resulted in a much slower reaction rate due to the longer lifetime of $C_5D_9^+$ by a factor of 5.

It should be noted that the above calculation *does* not take into account all of the isotope effects that may be important in the present experiment. For example, due to differences in zero point energy, C–D bond insertion has a slightly higher activation barrier than does C–H bond insertion. The calculated rate for decomposition of $V(C_4D_{10})^+$ assuming an activation barrier of 20.5 kcal/mol is also indicated in Figure 6. It can be seen that when this factor is included, the bond insertion rate for the adduct with deuterium-labeled *n*-butane-d_{10} is approximately 4 times slower than for the undeuterated adduct. This is in excellent agreement with the experimental ratio of lifetimes, 4.5. Recall that in modeling the dissociation reaction, it was assumed that the rate-limiting step was the initial C–H or C–D bond insertion by V^+. This choice was made based on considerations of the bonding to V^+ as discussed below.

In our simplified analysis, we have not considered the dissociation of the adduct to regenerate the reactants (M^+ and C_4H_{10} in Scheme III). The rate of this process may also exhibit pronounced isotope effects. As noted in the results section, the total cross sections for the sum of product and adduct formation in the case of *n*-butane and *n*-butane-d_{10} reacting with V^+ are equal to the theoretical limit for the collision cross section. Hence, in this system, the back reaction of the adduct to regenerate the reactants can be ignored, and the simplified kinetic scheme is appropriate.

Description of the Bonding to V^+ and Ti^+. The ground electronic states of Ti^+ and V^+ are derived from $4s^13d^2$ and $3d^4$ electronic configurations, respectively.[14] Recent calculations have shown that the diatomic metal hydrides of these metal ions utilize metal orbitals which are 40% d in character and 60% s and p in character.[36] Because s–d hybrid orbitals are used in the formation of the first M^+–H bond, to a first approximation, the second M^+–H bond in MH_2^+ will also be an s–d hybrid with an "inherent" bond energy comparable to that of the first. The inherent bond energy is defined here as the actual bond energy plus the promotion energy required to excite the metal ion to a configuration favorable for bonding. The promotion energy includes any exchange energy lost in forming the bond.

The inherent bond energies of MH^+ have been calculated to be 61 kcal/mol for both Ti^+ and V^+, by using the simplification that a pure s orbital is used in the formation of the bond.[36] To calculate the promotion energy necessary for MH^+ to bind an additional hydrogen atom, the assumption is made that the second bond uses a pure d metal orbital for bonding. Thus, instead of calculating the bond energies by using two s–d hybrid bonds, the bond energies are calculated by using one pure s bond and one pure d bond. The inherent strengths of the pure s and d bonds are taken to be equal to the inherent strength of an s–d hybrid bond. To promote TiH^+ from the ground $^3\Phi$ state to a state favorable for bonding requires the loss of one-half of a d–d exchange term or 8 kcal/mol.[37] In order to promote VH^+ from

(32) Miasek, P. G.; Harrison, A. G. *J. Am. Chem. Soc.* **1975**, *97*, 714.
(33) Robinson, P. J.; Holbrook, K. A. "Unimolecular Reactions"; Wiley: New York, 1972.
(34) Shenianouchi, T. "Tables of Vibrational Frequencies"; NSRDS-NBS 39, June 1972. The calculations were relatively insensitive to the actual frequencies chosen within the constraint of a frequency factor of 10^{13} s^{-1}.
(35) Bowers, M. T.; Elleman, D. D.; Beauchamp, J. L. *J. Phys. Chem.* **1968**, *72*, 3599.
(36) Schilling, J. B.; Goddard, W. A., III; Beauchamp, J. L. *J. Am. Chem. Soc.* **1986**, *108*, 582.
(37) The d–d exchange energy for the s^1d^2 configuration of Ti^+ is K_{d-d} = 16.5 kcal/mol. The d–d exchange energy for the s^1d^3 configuration of V^+ is K_{d-d} = 18.2 kcal/mol. Schilling, J. B., work in progress.

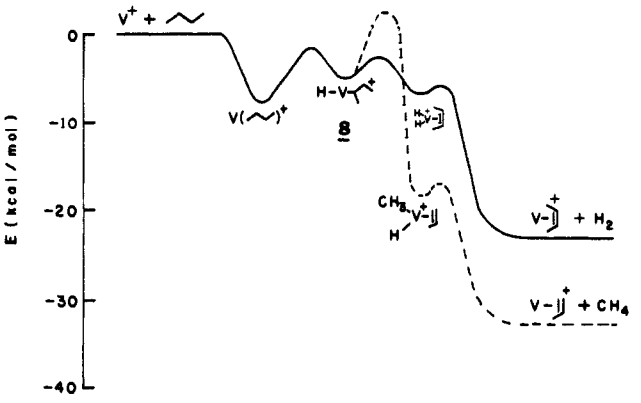

Figure 7. A simplified potential energy diagram for the reaction of V^+ with *n*-butane. The energies of the reaction intermediates were estimated by using the values discussed in the text. The strength of the V^+–olefin bonds was taken to be 50 kcal/mol, as suggested for $V-C_2H_4^+$ in ref 8.

the ground $^4\Delta$ state to a state favorable for bonding requires the loss of one d–d exchange term or 18 kcal/mol.[37] An estimate for the *second* bond energy, $D(MH^+-H)$, can be obtained from the inherent bond energy, less the promotion energy. This results in a second bond energy of 61 − 8 = 53 kcal/mol for Ti^+ and 61 − 18 = 43 kcal/mol for V^+. Thus, the sum of the first and second bond energies for MH_2^+ are 108 and 91 kcal/mol for Ti^+ and V^+, respectively. A more useful quantity for C–H bond activation is the sum of the two bonds in $R-M^+-H$. Using the values for M^+-CH_3 in Table I results in the sum of the two bonds being 109 and 93 kcal/mol for Ti^+ and V^+, respectively. Note that the estimates for the binding energies to Ti^+ are in excellent agreement with the lower limit $D(Ti^+-2CH_3) \geq 112$ kcal/mol determined from the reaction with *n*-butane to form $Ti(CH_3)_2^+$.

Typical C–H bond energies for alkanes are in the range 92–98 kcal/mol.[38] It is thus apparent that the bond energies to Ti^+ are more than sufficient to allow for exothermic C–H bond activation. The case for V^+, however, is not so clear. From the estimates made above, it appears that V^+ should be able to activate only tertiary C–H bonds. Assuming that the bond to an alkyl group is stronger than to a methyl group (by 5 kcal/mol) results in V^+ being just barely able to activate secondary C–H bonds. This could explain why V^+ *does not react* with 2,2-dimethylpropane. Only primary C–H bond insertions or C–C bond insertions are possible with 2,2-dimethylpropane, neither of which may be facile processes for V^+. This is also supported by the extensive loss of H_2 from *n*-butane-1,1,1,4,4,4-d_6, perhaps indicating preferential attack at the secondary C–H bonds.

The impact of weak bonds to V^+ on the reactivity of this metal ion can be seen from the qualitative potential energy surface for the 1,2-elimination of H_2 from *n*-butane illustrated in Figure 7. This potential energy surface explains the special features of the V^+ reactions observed in this study. The initially formed insertion adduct **8** is very high in energy. The noninserted adduct ion may have 10–20 kcal/mol of excess energy due to electrostatic interactions. Thus the inherent activation barrier for C–H bond insertion is probably higher than for β-H transfer. The frequency factors for the two processes should be somewhat similar, resulting in C–H bond insertion as the slow step in the overall dissociation.

Because of the energy of intermediate **8** is so high, if β-methyl transfer has a somewhat higher intrinsic barrier than β-H transfer, then the former process would almost certainly be energetically unreasonable. This is indicated by the dashed line in Figure 7. This may explain the lack of reaction of V^+ with 2,2-dimethylpropane. This also may be partially responsible for the lack of alkane loss products observed in general.

Conclusion

The reactions of Ti^+ and V^+ with alkanes are dominated by the loss of one or more molecules of hydrogen, similar to the reactions observed for Ru^+ and Rh^+. Alkane loss reactions are also observed for Ti^+ but may be due to electronically excited state reactions. It is proposed that both Ti^+ and V^+ dehydrogenate alkanes by predominantly 1,2-mechanisms, where some 1,3-elimination occurs for the reaction of Ti^+ with *n*-butane. Although there is much similarity in the reactions of Ti^+ and V^+ with Ru^+ and Rh^+, there are also important differences, especially for V^+. Extensive adduct formation and a large deuterium isotope effect for V^+ are consistent with much longer adduct lifetimes for this metal ion than for Ti^+, Ru^+, and Rh^+. The measured dissociation rate of the V^+ adducts with *n*-butane is 100 times slower than for Ti^+. It is suggested that V^+ cannot form two strong σ bonds due to the $3d^4$ electronic configuration of ground-state V^+. This makes insertion into C–H bonds much more difficult than for the other metal ions and may in fact prevent primary C–H bond insertions. This results in higher activation barriers and the formation of relatively long-lived intermediates. Because the lifetime of the adduct ion is comparable to the ion flight time to the detector, a large deuterium isotope effect is observed in the reactions of V^+ with labeled alkanes. The occurrence of these isotope effects is supported by the results of RRKM calculations for C–H and C–D bond insertions for V^+ interacting with C_4H_{10} and C_4D_{10}. These isotope effects are not observed for the reactions of Ti^+.

Acknowledgment. This work was supported by the National Science Foundation under Grant CHE-8407857.

Registry No. Ti^+, 14067-04-0; V^+, 14782-33-3; $TiCl_4$, 7550-45-0; $VOCl_3$, 7727-18-6; D_2, 7782-39-0; CH_3CD_3, 2031-95-0; $H_3CCD_2CH_3$, 2875-95-8; $D_3CCD_2CD_3$, 2875-94-7; $D_3C(CH_2)_2CD_3$, 13183-67-0; $D_3C(CD_2)_2CD_3$, 7582-04-9; $(H_3C)_2CDCH_3$, 13183-68-1; $(H_3C)_3CCH_3$, 463-82-1; $H_3C(C(CH_3)_2)_2CH_3$, 594-82-1; C_2H_6, 74-84-0; C_3H_8, 74-98-6; C_4H_{10}, 106-97-8; *i*-C_4H_{10}, 75-28-5.

(38) McMillen, D. F.; Golden, D. M. *Ann. Rev. Phys. Chem.* **1982**, *33*, 493.